Journal of Hydrology 568 (2019) 501–516

Contents lists available at ScienceDirect

Journal of Hydrology

journal homepage: www.elsevier.com/locate/jhydrol

Research papers

Impacts of groundwater depth on regional scale soil gleyization under changing climate in the Poyang Lake Basin, China

Yun Yang[a,c,*], Zhenchen Wang[b], Yueqing Xie[b], Behzad Ataie-Ashtiani[c,d], Craig T. Simmons[c], Qiankun Luo[e], Gan Chen[b], Qi Zhang[f], Jianfeng Wu[b,*], Jinguo Wang[a], Jichun Wu[b]

[a] School of Earth Sciences and Engineering, Hohai University, Nanjing 210098, China
[b] Key Laboratory of Surficial Geochemistry, Ministry of Education, Department of Hydrosciences, School of Earth Sciences and Engineering, Nanjing University, Nanjing 210023, China
[c] National Centre for Groundwater Research and Training and College of Science & Engineering, Flinders University, Adelaide, South Australia 5001, Australia
[d] Department of Civil Engineering, Sharif University of Technology, Tehran 1458889694, Iran
[e] School of Resources and Environmental Engineering, Hefei University of Technology, Hefei 230009, China
[f] State Key Laboratory of Lake Science and Environment, Nanjing Institute of Geography and Limnology, Nanjing 210008, China

ARTICLE INFO

This manuscript was handled by G. Syme, Editor-in-Chief, with the assistance of Xiaodong Zhang, Associate Editor

Keywords:
Soil gleyization
Groundwater depth
Numerical modeling
Climate change
Poyang Lake

ABSTRACT

Various natural and anthropogenic factors affect the formation of gleyed soil. It is a major challenge to identify the key hazard factors and evaluate the dynamic evolutionary process of soil gleyization at a regional scale under future climate change. This study addressed this complex challenge based on regional groundwater modelling for a typical agriculture region located in the Ganjiang River Delta (GRD) of Poyang Lake Basin, China. We first implemented in-situ soil sampling analysis and column experiments under different water depths to examine the statistical relationship between groundwater depth (GD) and gleyization indexes including active reducing substance, ferrous iron content, and redox potential. Subsequently, a three-dimensional groundwater flow numerical model for the GRD was established to evaluate the impacts of the historical average level and future climate change on vadose saturation and soil gleyization (averaged over 2016–2050) in the irrigated farmland. Three climate change scenarios associated with carbon dioxide emission (A1B, A2, and B1) were predicted by the ECHAM5 global circulation model published in IPCC Assessment Report (2007). The ECHAM5 outputs were applied to quantify the variation of groundwater level and to identify the potential maximum gleyed zones affected by the changes of meteorological and hydrological conditions. The results of this study indicate that GD is an indirect indicator for predicting the gradation of soil gleyization at the regional scale, and that the GRD will suffer considerable soil gleyization by 2050 due to fluctuations of the water table induced by future climate changes. Compared with the annually average condition, the climate scenario B1 will probably exacerbate soil gleyization with an 8.8% increase in total gleyed area in GRD. On average, the highly gleyed areas will increase in area by 29.7 km^2, mainly on the riverside area, and the medium-slightly gleyed area will increase by 19.2 km^2 in the middle region.

1. Introduction

Soil gleyization is a process of soil formation due to lack of oxygen (under an anaerobic environment) that results in the development of a gley horizon in the soil profile. This process is highly dependent on poor drainage conditions that result from land depressions with low topographic elevation, continuous water recharge with water-logged conditions, impervious soil parent materials, and lack of aeration (Brammer and Brinkman, 1977; Lin et al., 2007; Singh and Chandran, 2015). The gleyed soil is oxygen-poor and contains much reductive material, which weakens the biological activity of soil, inhibits the mineralization of organic matter, restricts plant root growth, and results in late maturity and low yield grain crops (Rowell, 1988; Verheye, 2007; Liu et al., 2015). Gleyed soils are widespread across the world, such as in the North German Plain (German Soil Science Society, www.dbges.de; Burbaum et al., 2016), New Zealand wetlands (Webb and

* Corresponding authors at: School of Earth Sciences and Engineering, Hohai University, Nanjing 210098, China (Y. Yang). School of Earth Sciences and Engineering, Nanjing University, Nanjing 210023, China (J.F. Wu).
E-mail addresses: yy_hhu@hhu.edu.cn (Y. Yang), behzad.ataieashtiani@flinders.edu.au (B. Ataie-Ashtiani), craig.simmons@flinders.edu.au (C.T. Simmons), luoqiankun.kun@163.com (Q. Luo), qzhang@niglas.ac.cn (Q. Zhang), jfwu@nju.edu.cn (J. Wu), wang_jinguo@hhu.edu.cn (J. Wang), jcwu@nju.edu.cn (J. Wu).

https://doi.org/10.1016/j.jhydrol.2018.11.006
Received 21 June 2018; Received in revised form 17 September 2018; Accepted 2 November 2018
Available online 15 November 2018

Lilburne, 2011), Scotland (Brown, 2017), and the middle reaches of the Yangtze River, China (Pan, 1996). In the middle reaches of the Yangtze River, about 30–40% of total paddy soil has suffered from gleyization and its extent is undergoing dramatic changes due to global environmental changes (Ye et al., 2011). Therefore, it is important to identify the key hazard factors for soil gleyization and evaluate the dynamic evolutionary process of gleyization at the regional scale. In addition, identification of the potential maximum gleyed zones that are likely to be affected by changes in meteorological and hydrological conditions are of great importance for regional land resource planning and management.

Soil gleyization takes hundreds of years and is still developing due to changes in many controlling factors including climate, land use, and parent material. Climate is one of the most important factors affecting the soil saturation conditions (DEFRA, 2005; Karmakar et al., 2016) and hence soil gleyization. Evaluation of the dynamic evolutionary process of gleyization at the regional scale under changing climate has posed major challenges. However, relatively few studies have undertaken qualitative assessments at the regional scale (Lai et al., 1989; Lin et al., 2009) and quantitative analysis at the field scale (Schlichting and Schwertmann, 1973; Pan, 1996). Pan (1996) determined the quantitative evaluation indexes of soil gleyization through principal component analysis (i.e., active reducing substance (ARS) (cmolc/kg), ferrous iron content (Fe^{2+}) (cmolc/kg), and redox potential (Eh) (mV)) in the middle reaches of the Yangtze River. The use of these indexes can elucidate vadose saturation conditions in the soil, which result in the cut-off of oxygen supply and the occurrence of reducing reactions. Lin et al. (2009) suggested that under the necessary conditions (e.g., depressions in the land surface, water-logged conditions, impervious soil media, and a lack of aeration), groundwater level or depth is an indirect indicator for predicting soil gleyization. This conclusion provides us with new directions for the study of the evolutionary tendency of gleyed soil based on establishing the relationship between groundwater depth (GD) and soil gleyization, in which the regional variable of GD can be predicted by groundwater modelling. Furthermore, the successful selection and implementation of engineering measures to mitigate soil gleyization of low-lying and water-logged reclaimed farmland will also require a sound knowledge of soil forming processes and the hydrogeological processes governing the groundwater flow system. Therefore, in this study, we attempted to establish a statistical relationship between GD and gleyization indexes based on the physical and chemical data of soil collected by field soil sampling, laboratory testing, and soil column experiments.

Poyang Lake is the largest freshwater lake in China. Its major functions include ecological security, hydrological adjustment, and climate regulation. These are important for the Jiangxi provinces and municipalities in the middle and lower reaches of Yangtze River (Zhang et al., 2014). The Poyang Lake Basin (PLB) is the most densely populated and economically developed area in Jiangxi Province, and is a major rice production area for the province and more generally, the nation, with 19.08% of the total rice production in Jiangxi (Li et al., 2012; Zhang et al., 2017). As the PLB lies in the low-lying, rainy and humid region surrounded by a complicated surface water system, the surface water in the lake and rivers has a close hydraulic connection with the shallow groundwater (Zhan et al., 2016). However, the hydrological process in PLB has experienced substantial changes due to natural variables and human activities and will subsequently change with future natural or man-made disturbances (Ye et al., 2011, 2013; Mei et al., 2015). Liu and Wu (2016) indicated that in the past decade, the PLB was six times more likely to suffer droughts due to decreased inflow, increased outflow, reduced precipitation and increased evapotranspiration. Lai et al. (2014) studied the impoundment effects of the Three-Gorges-Dam on flow regimes, which significantly reduces run-off in the Yangtze River during the dry season (September to the next February), resulting in increasing lake discharge to Yangtze River, thus prolonging the dry period and threatening the regional ecological environment. Ye et al. (2011) implemented a modeling study to examine changing water levels in the Poyang Lake due to future climate change. The results demonstrated that the changing monthly catchment inflow resulted in an increase of the lake level from February to July and a reduction from September to the next February. The spatio-temporal variability of hydrologic processes in watersheds caused by climate change will change the groundwater level dynamics, which further modifies the soil physical and chemical properties, as well as the agronomical characteristics, and affects a series of soil process.

Hundreds of studies on surface water and groundwater interactions in PLB have been conducted since the late 1990′s (e.g., Wagner et al., 2016; Zhan et al., 2016); however, to our knowledge, no studies have implemented regional groundwater modeling to evaluate groundwater dynamics regimes. A regional groundwater flow model will help land resource and water resource managers better understand the interrelated groundwater and surface water systems and the effects of groundwater level variation under different hydrological processes (Balbarini et al., 2017; Havril et al., 2017; Epting et al., 2018). The objective of our study was to quantify the possible impacts of climate change on soil gleyization on a regional scale in the PLB. We therefore constructed a three-dimensional numerical model for shallow aquifers to simulate the hydrogeological system behavior for changing boundary conditions and to quantify the dynamic evolutionary process of soil gleyization based on the resultant groundwater fluctuations. The innovative aspects of this research were the exploration of the formative mechanism of soil gleyization at the regional scale by statistically analyzing the relationship between GD and gradation of soil gleyization based on soil sampling analysis and column experiments. In addition, the groundwater dynamics were quantified using groundwater modeling under a changing climate. We believe that this study provides an important new laboratory case study. Furthermore, the impact of groundwater dynamic patterns on the PLB soil gleyization due to future climate change could be applied to other low-lying deltas in the middle and lower reaches of Yangtze River and other parts of the world with similar hydrogeological conditions.

2. Methods

2.1. Study area

2.1.1. Description of study area

Poyang Lake, the largest freshwater lake in China, is located in the middle reaches of the Yangtze River with a catchment area of > 162,000 km^2. Five tributaries run separately from the east (Rao River), south (Ganjiang River, Fu River, and Xinjiang River), and west (Xiu River) into the lake through the PLB and forms fluvial-deltas plain around the lakeshore area. The Ganjiang River Delta (GRD) is the largest scale of the alluvial-lacustrine low-lying area in the PLB, was selected as the detailed evaluation area in this study. We focus on the low-lying agriculture catchment of GRD for several reasons: (1) the GRD, a closed and independent hydrogeologic area, is already being threatened by a relatively high degree of soil gleyization in the middle reaches of the Yangtze River; (2) the GRD is rich in agricultural resources (Fig. 1) and intensive socioeconomic activities (Torbick et al., 2011) and it is thus urgent at the national level to conduct scientific land resource planning and management for further climate change; (3) the formative mechanism of soil gleyization in this region possess direct or indirect relation with the hydrogeological system (Lin et al., 2009); and (4) an enormous amount of different types of hydrological and hydrogeological data (conducted by geological survey; Geological Data Information Network of Jiangxi Province, http://www.jxgtt.gov.cn/dzzlg/Index.shtml; National Meteorological Information Center, http://www.nmic.cn/web/index.htm) has allowed us to establish a three-dimensional groundwater model to evaluate the processes in the alluvial-lacustrine groundwater system.

The Ganjiang River is the largest river in the GRD flowing north

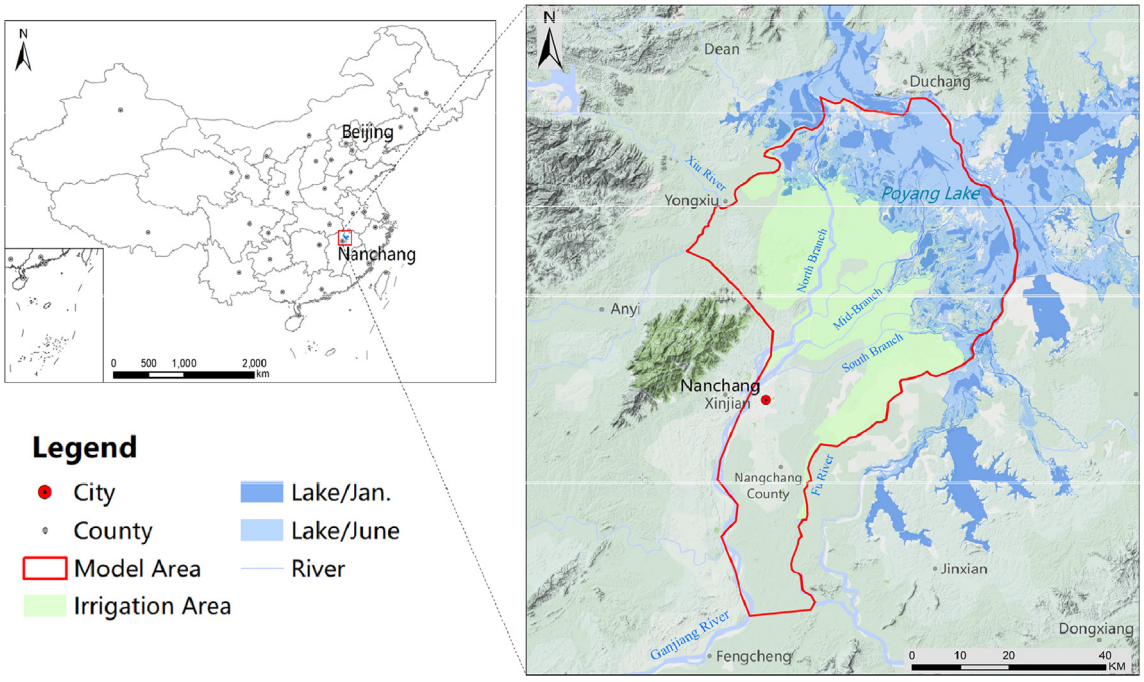

Fig. 1. The geographical extent, topography, stream systems, and irrigation region in the study area.

through Nanchang City, which is the economic and administrative center of Jiangxi Province. As shown in Fig. 1, the main branch of Ganjiang River is divided into the north branch, middle branch, and south branch before finally entering into Poyang Lake. The study area receives about 1343–1834 mm of precipitation and loses about 1044 mm through surface evaporation per year (1960–2014 average; National Meteorological Information Center). It is therefore a humid environment (Zhang et al., 2014). In general, annual precipitation consists of dense rain in the rainy season from April to August accounting for 74% of the total rainfall and a small fraction occurs from September to the following March. Groundwater withdrawals have increased since the 1960s. By the 1990s, with significant continued groundwater extraction, a large cone of depression had formed in Quaternary shallow aquifers beneath Nanchang City. In the last 10 years, the local enforcement of pumping limits has restored groundwater levels by as much as 5.6 m in the most depressed area. According to groundwater extraction statistics, 89.7% of total groundwater extraction is dispersedly extracted for irrigation and domestic usage and 10.3% of the total amount is associated with centralized groundwater pumping in Nanchang City for industrial use (Xiao et al., 2001).

The gleyization of irrigated farmland is a serious soil degradation problem in this region. According to an investigation of farmland soil, in the 1950s, small-scale primary soil gleyization began to place in the low-lying lakeside areas and some cold-invasive paddy fields in the surrounding hilly areas. From the 1950s to the 1980s, secondary gleyization of paddy soil became serious and the gleyed soil area accounted for > 15% of the total area of paddy field in the GRD (Lai et al., 1989). There are three main reasons for the formation of soil gleyization in this area: (1) favorable hydrogeological conditions for soil gleyization with poorly drained conditions, water-logged conditions, and a reductive soil environment; (2) land reclamation of meadow soil into paddy soil and further development of gleyed paddy soil; and (3) groundwater table rise caused by regional scale water conservation measures since 1970 and regularization and networking of the river system (Jiangxi Institute of Red Soil, 1987). Some paddy soils are in a saturated condition perennially, which result in a loss of oxygen supply and the occurrence of reducing reactions. In the last 10 years, the process of soil gleyization has been effectively controlled as the result of agricultural management measures such as establishment of a ditch drainage network system, auxiliary treatment with continuous flooding, and ridge agriculture (Jiangxi Institute of Red Soil, 1987; Shiratori et al., 2007; Li et al., 2015; Clagnan et al., 2018).

2.1.2. Hydrogeology

The GRD can be considered to be a relatively independent hydrogeological unit covering 3649 km^2 of the western part of the PLB. The regional boundaries of the study area follow the edges of Poyang Lake and its branches (Fig. 2). For example, the northern boundary is the Xiu River, the southeastern boundary is the Fu River, the western boundary is the Ganjiang River, and the eastern boundary is Poyang Lake. Principal surficial geological units within the study area include the Holocene and upper Pleistocene unit, and the middle-lower Pleistocene unit, both mainly made of fluvial facies alluvium and fluvial-Lacustrine facies alluvium in the Quaternary age. The Holocene and upper Pleistocene unit comprises two distinct sedimentary formations. The upper layer of this geologic formation is the sandy silt clay, mainly distributed in the surface of the fluvial-deltas plain and the underlying layer is coarse sand and gravel, comprising the alluvial aquifer, which is the principal aquifer in the study area. Aquifer thickness increases from upstream to downstream in the Ganjiang-Fu River plain, locally up to thickness of 36 m. The aquifer has a high productivity with a potential yield of > 17,200 m^3/day per well from southern Xiangtang Town to northern Nanchang City (Holocene and Upper Pleistocene unit (S) in Fig. 2) and a moderate productivity with a yield of 3456–10,264 m^3/day per well in other areas (Holocene and Upper Pleistocene unit (M) in Fig. 2). The middle-lower Pleistocene unit consists of red clay gravel, residual slope deposit, glacial clay, and reticulated red clay, and is distributed in the border area of the fluvial-deltas plain, especially in the hillock plain area (e.g., in Xinqizhou in the northern part of Nanchang City). This unit has a variable thickness from 3 to 15 m and a low productivity with a potential yield of 35–166 m^3/day per well. The older geological units are the Tertiary and Cretaceous red clastic rock formation underlying the alluvial aquifer and forming a no-flow bottom boundary. The surficial hydrogeology (Fig. 2) was mapped by combining multiple data sets from the Geological Data Information Network of Jiangxi Province (http://www.jxgtt.gov.cn/dzzlg/Index.shtml) and the geological survey (1986–1988) conducted by the Jiangxi Geology &

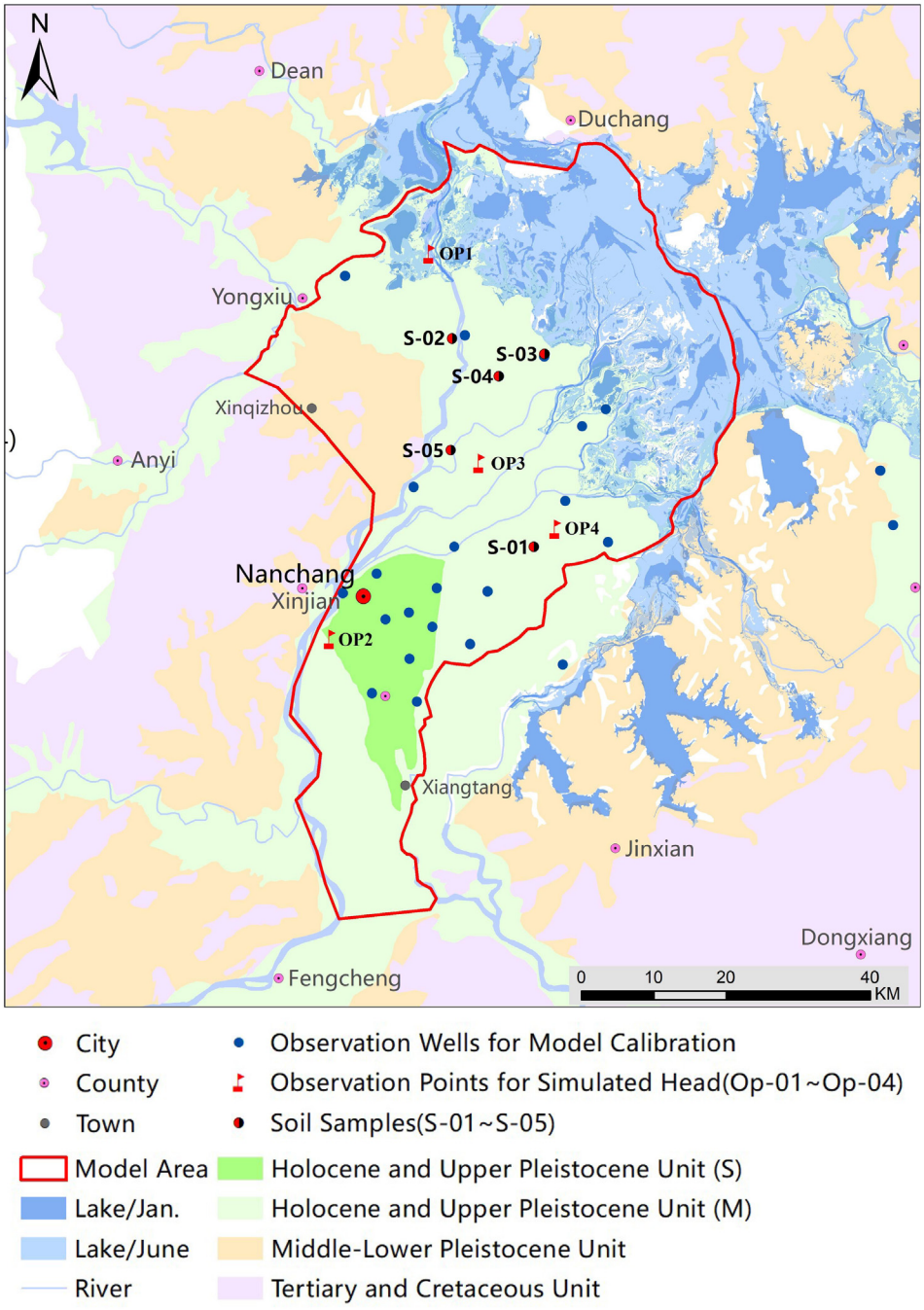

Fig. 2. Surficial hydrogeology, locations of soil sampling and observation wells in the study area (modified from Li et al., 2008).

Mineral Exploration Bureau (Guo and Chen, 2008).

In this region, the five tributaries and Poyang Lake are deeply downcut with an average river-bed elevation of 3–7 m and lake channel bed elevation of 4–6 m above sea level based on the 90 m STRM_Version1 (http://dds.cr.usgs.gov/srtm/) digital elevation model (DEM) data. In addition, high linear correlation coefficients (R_{SG}) were determined between groundwater level and nearby surface water level based on observation data from three stages of groundwater and surface water monitoring (1986–1988) (Guo and Chen, 2008). The average R_{SG} was 0.70 at Waizhou station (Ganjiang River), 0.69 at Zajing station (Xiu River), 0.78 at Lijiadu station (Fu River), 0.81 at Wucheng station (junction between Ganjiang River and Poyang Lake), and 0.77 at Kangshan station (interaction joint of Fu River and Poyang Lake). Based on the above DEM data and the dynamic relationship between surface water level and groundwater level, we conclude that the channels of the Ganjiang River, Xiu River, Fu River, and Poyang Lake cut through the alluvial aquifer. The area enclosed by these water bodies is an independent hydrogeological unit surrounded by specified head boundaries. Local bodies of surface water and their seasonal variations strongly affect the direction and magnitude of groundwater flow. Therefore, groundwater and river water exchange seasonally, groundwater flowing into rivers along the exposing aquifers in the dry and flat seasons and river water also recharging aquifers, replenishing the aquifer in the wet season.

2.2. Measurement methods for identifying gleyization

In this region, the extent of soil gleyization can be broadly classified into four types: highly gleyed, medium gleyed, slightly gleyed, and ungleyed (Lai et al., 1989; Pan, 1996). The main characteristics of each

type are as follows: (1) Highly gleyed type: the gley horizon covers the whole soil profile, and poor drainage conditions including surface water-logged soil, groundwater saturated, low temperature and poor ventilation of soil, a large amount of toxic reducing substance in strong reduction state, and extremely negative effects on plants growth. (2) Medium gleyed type: the gley horizon exists below the plough layer (a depth of 20–40 cm below the ground surface), oxidation environment in the upper layer, poor ventilation and reduction state in middle layer generating a large amount of toxic reducing substance, and interference with plant root development. (3) Slightly gleyed type: gley horizon declines (about 60 cm below the ground surface) with an increasingly deep groundwater level, and well-drained conditions, but inundated by intermittent flooding, with less effect on plant growth. (4) Ungleyed type: the gley horizon does not exist in the soil profile, oxidation environment exists throughout the whole soil layer with a much deeper groundwater level and far superior drainage conditions. To explore the formative mechanism of soil gleyization and identify the impacts of GD on soil gleyization at a regional scale, we first describe the principal indexes for predicting the different type of soil gleyization, and then develop the measurement methods including soil sampling analysis and column experiments for testing each index for different depths to water table.

2.2.1. Identification indexes

The formation of soil gleyization is characteristic of poorly drained conditions in the middle reaches of the Yangtze River. As the groundwater slowly saturates the soil, the soil environment converts to a reduced state when it loses oxygen and it is acidified by effect of the organic matter. In reducing conditions, the iron and manganese compounds in the soil are reduced to mobilizable Fe^{2+} and Mn^{2+} depending on the existing redox potential Eh, which is defined as the potential between a couple of oxidation-reduction electrodes measured in a galvanic cell against the standard hydrogen electrode (Fiedler et al., 2007). The Eh can be measured as an indicator of the relative abundance of oxidized and reduced substances. If the groundwater level is maintained constant throughout the year, reducing conditions predominate, generating more ARS including Fe^{2+} and Mn^{2+}, and gradually forming the gleyed horizon in the soil profile.

It is a fundamental issue to establish an identification index system for distinguishing different types of soil gleyization. Soil scientists have studied the description and prediction criteria for this issue from different perspectives for some time (Pu et al., 1994; Pan, 1996; Liu et al., 2015). Pan (1996) determined the quantitative evaluation indexes of soil gleyization by principal component analysis with 13 factors in the middle reaches of Yangtze River. The results indicated that the cumulative variance contribution rates of three principal factors, the total amount of ARS (cmolc/kg), the quantity of Fe^{2+} (cmolc/kg), and Eh (mV), explained 79.3% of observed differences and hence distinguishing various gleyization types. These three indexes contain most of the soil information for determining the soil gleyization classification. The ranges of three principle indexes for the gradation of soil gleyization are given in Table 1. This indexing system in combination with ARS, Fe^{2+}, and Eh has been widely applied in the fluvial-alluvial plains in the middle reaches of the Yangtze River, such as the Four Lake Region (Chang Lake, San Lake, Bailu Lake, and Hong Lake) in the Jianghan Plain, the Dongting Lake Basin, and the PLB.

Table 1
The criteria of three principle indexes for gradation of soil gleyization (Pan, 1996).

Index	Highly gleyed	Medium gleyed	Slightly gleyed	Ungleyed	Contribution rate (%)
ARS (cmolc/kg)	> 3.0	0.7–3.0	0.1–0.7	< 0.1	47.4
Fe^{2+} (cmolc/kg)	> 2.5	0.5–2.5	0.05–0.5	< 0.05	17.5
Eh (mV)	< 100	100–300	300–500	> 500	14.4

2.2.2. In-situ sampling and testing

According to the geological survey, groundwater monitoring, and land information provided by the Jiangxi Institute of Red Soil, 5 soil sampling sites (S-01–S-05) have been selected and their locations are as shown in Fig. 2. The soil samples are collected from soil depths of 0–30 cm (within the soil plough layer), and 30–60 cm (below the plough layer) at each site once every month for a whole year as shown in the schematic diagram in Fig. 3(a). Representative soil samples were obtained using a core sampling tool and a total of 120 soil samples were collected to test the three key indexes of gleyization at different depths of the water table below the ground surface. In each sample site, a fully penetrating well was installed in the upper unconfined layer and GD in the well was monitored monthly, at the same time with soil sampling. The annual average GDs at the 5 sampling sites were 0, 30, 50, 70, and 90 cm, as shown in Fig. 3(b).

The Eh of the sample sites were measured in-situ. The measurements are actually recordings of voltage over 10 mins when a steady value was obtained between a reference electrode and a sensor electrode inserted into the soil. The Oxidation–Reduction potentiometer (Orion 9180BN) was used to check the Eh in the two layers for 3–4 times to obtain mean Eh values. The moist field soil was divided into two subsamples which were immediately processed by vacuum-packaging and transported to the laboratory to analyze the content of ARS and Fe^{2+} within 3 days. Reducing substances were extracted by 50 mL of 0.1 mol/L $Al_2(SO_4)_3$ solution (pH 2.5). The ARS in the extracts of reducing substances include Fe^{2+} and organic compounds. The Fe^{2+} was determined calorimetrically by taking an aliquot of the extracts, and the ARS was determined by titration of an aliquot of the extract with $KMnO_4$ solution after acidification with H_2SO_4 solution.

2.2.3. Laboratory experiments

The experimental design includes the main device of the soil column, water table control system and sampling and monitoring system. A schematic diagram of the experimental equipment is shown in Fig. 4. The test cylinder consists of a translucent acrylic tube 120 cm in height with a 40 cm internal diameter. The soil used in the column tests was undisturbed samples collected from the GRD and covered with paddy straw. The column was instrumented with 4 in-situ testing and sampling holes (L1, L2, L3, and L4, at depths of 10, 30, 45, and 55 cm, respectively) to measure the oxidation-reduction potential and take soil samples. The water pressure at the bottom of the gravel filter was generated using a constant head tank fed by a submersible pump from a large reservoir, so the water moved upward into the soil. The constant head tank was connected to a manually driven rolling wheel and was lifted to the given position over a period of about 3 days until the soil column was naturally saturated. A piezometric tube was installed at the bottom of the soil column to measure the total head of the saturated soil. Five different water table depths (with water table depths of 0, 20, 40, 60, and 80 cm) were established using control water valves, so that if the water table were to move upward above the specified height, internal runoff of excess water would be diverted into a collector. For each water table condition, Eh was measured through the sampling hole and the total amount of ARS and Fe^{2+} were obtained by sampling tests after the saturated soil column had settled in the laboratory for a period of 2 months at ambient room temperature.

In this study, soil gleyization due to the variation of the water table was studied by the above in-situ sampling analysis and laboratory experiments. The results were then used to establish a statistical relationship between GD and the gradation of soil gleyization.

2.3. Groundwater modeling

To quantify changes in the lakeside groundwater flow regime, we established a transient three-dimensional groundwater flow model

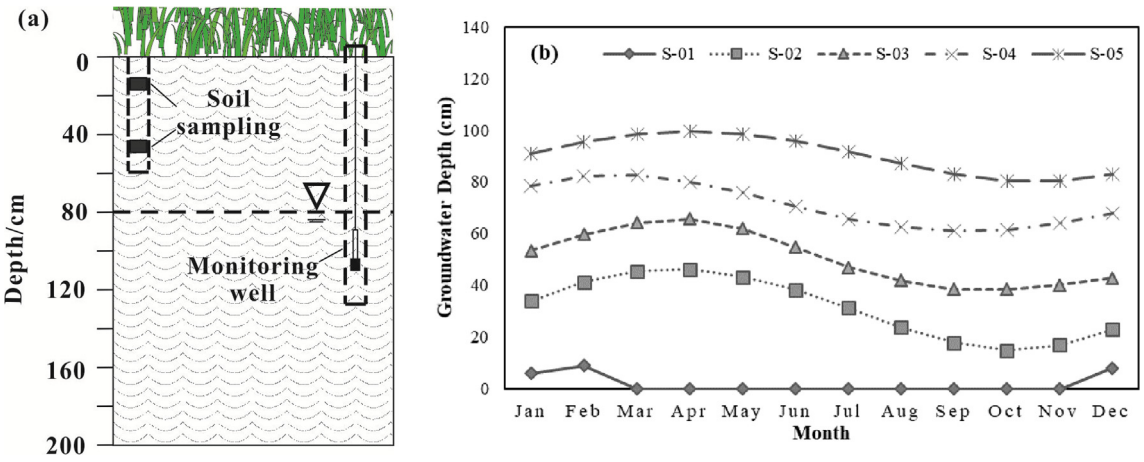

Fig. 3. Schematic diagram for soil sampling (a) and groundwater depths in the 5 soil sampling sites (b) during sampling period.

based on the widely used FEFLOW code (Diersch, 2014). FEFLOW enables modeling of surface water and groundwater interactions in saturated and unsaturated porous media. The groundwater modeling software combines GIS graphical features with finite element solution techniques.

2.3.1. Model setup

Based on stratigraphic records from 276 boreholes collected from the geological survey report by Zhang (2008), the groundwater model consists of two aquifers and a bedrock basement (Fig. 5). The upper aquifer (Layer 1) is an unconfined and low-permeability layer comprising fine-grained sediments (silty clay to silty loam). This layer is approximately 10–20 m thick and was largely formed from the Upper Pleistocene and Middle-lower Pleistocene to current Holocene. The lower aquifer (Layer 2) is a confined aquifer composed of mostly alluvial materials (sand and gravel). It was mainly deposited in a fluvial setting during the Holocene and Upper Pleistocene. The thickness of this layer increases from upstream to downstream (7–16 m in general and locally up to 20–36 m). The bedrock layer (Layer 3) represents the red clastic rock formation formed during the Tertiary and Cretaceous periods. The bedrock was treated as a zero permeability layer as no apparent joints and fissures were found.

Each water-bearing layer (Layer 1 and Layer 2) was divided into 7 zones (Fig. 6) based on surficial hydrogeological mapping (see above Fig. 2) and in-situ survey parameters collected from the Pumping Tests Report, an affiliated document of Investigation Report on Groundwater Resources (Guo and Chen, 2008). A total of 110 pumping tests were conducted in 1986–1988 throughout the region (Jiangxi Geology & Mineral Exploration Bureau, 1986–1988). Statistical analysis shows that the hydraulic conductivity differed significantly between Layer 1 and Layer 2 but did not differ significantly among different zones within each layer. Hence, we assigned the same range of hydraulic conductivity to all the zones within each layer as initial guesses (i.e., 0.005–5.0 m/d for Layer 1 and 8–150 m/d for Layer 2). Other parameters (e.g., porosity and specific storage (S_S), specific yield (S_y)) required model parameters. The initial parameter ranges were obtained from the geological survey by Wei et al (2005) on the basis of established aquifer characteristics. The actual hydrogeological parameters for different zones were optimized through model calibration as described below.

The model domain was bounded by Poyang Lake and the tributary streams (Fig. 1), which were assigned as specified head boundary

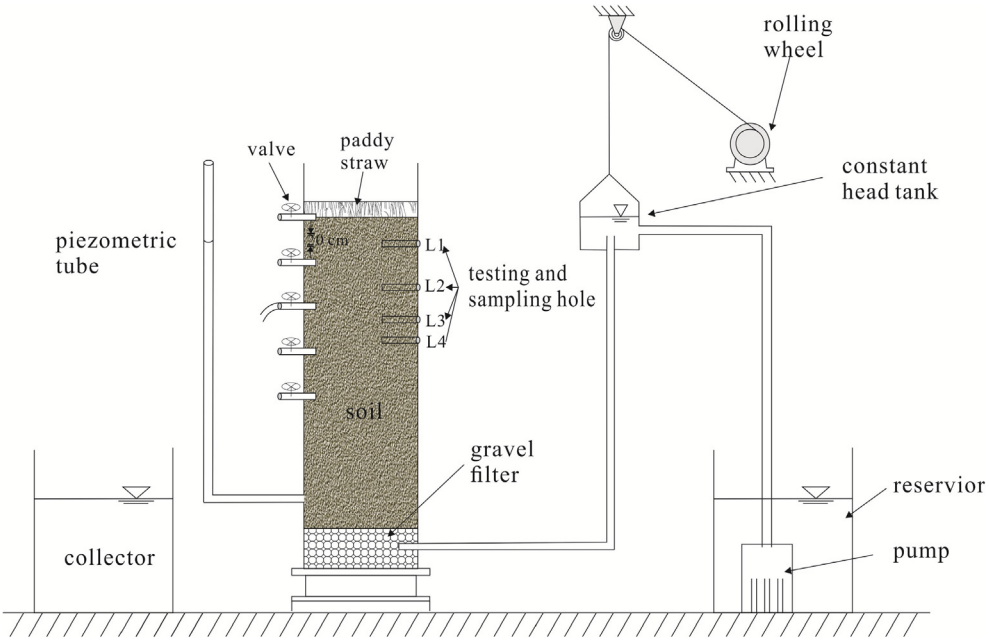

Fig. 4. Schematic diagram of experimental apparatus for detecting gleyization indexes under different saturations.

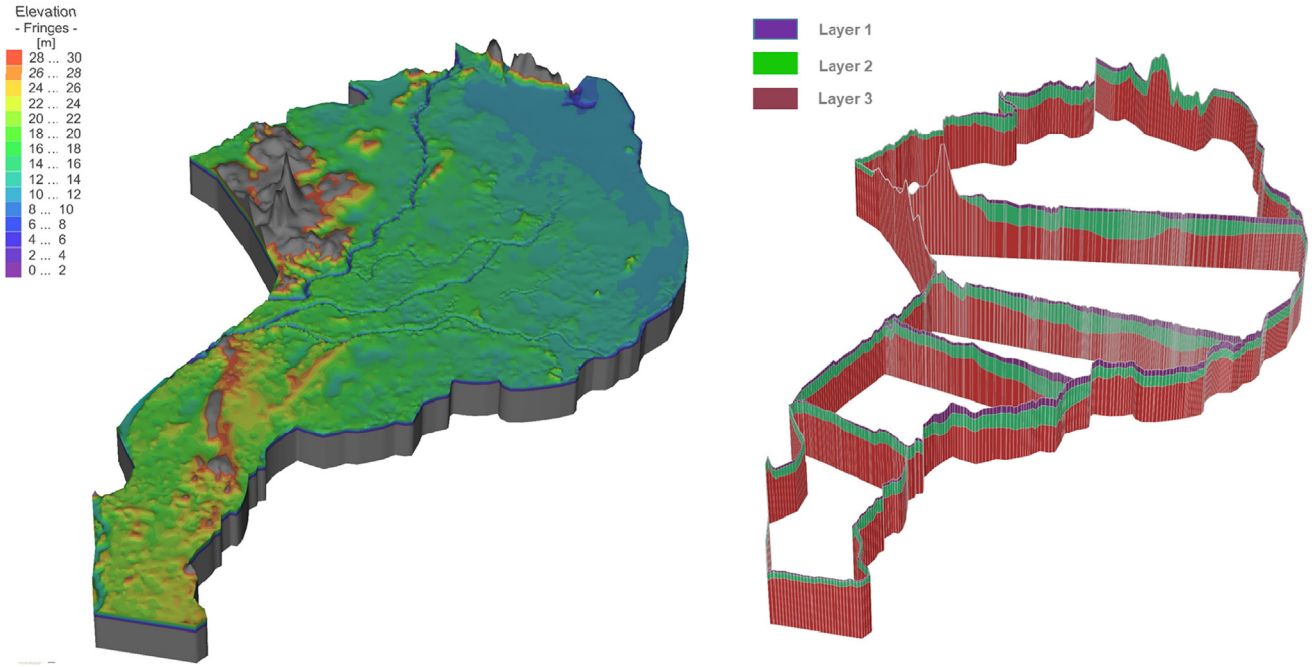

Fig. 5. Three-dimensional geological model and geological profiles across the study area.

conditions (see Section 2.2). In comparison to river boundaries, the northern to northeast boundaries were strongly affected by the size of Poyang Lake. Monthly Landsat remote sensing images (2004–2016) show that the lake size changed dramatically between wet and dry seasons (Fig. 1). Hence, the Poyang Lake boundary was assigned as a specific head boundary condition but the size and head were adjusted monthly in accordance with the monthly Landsat remote sensing images (2004–2016). Constant heads along the river and lake boundaries were interpolated between monitored transient water levels recorded at six gauging stations (e.g., the northern boundary of Xiu River between Zajin and Wucheng stations; western boundary of Ganjiang River between Waizhou and Wucheng stations; southwestern boundary of Fu River between Lijiadu and Kangshan stations; the Poyang Lake between Kangshan, Tangyin, and Wucheng stations) (Jiangxi Hydrology Information Center for the period 1960–2014). The top of the model was assigned as flux boundary condition to represent groundwater recharge derived from precipitation infiltration. The fluxes were treated as a model calibration parameter for net recharge rate. The bottom of the model was assigned as a zero permeability boundary condition as the bedrock was simulated as the bottom layer.

The three-dimensional groundwater flow model was discretized into 34,951 triangular prismatic mesh elements with 22,262 nodes for each layer in the horizontal orientation. The mesh was moderately refined along the river and lake boundaries, interior stream nodes and also in the neighborhood of observation wells. The lateral size of the mesh elements varied from 100 to 680 m. Vertically, the model extended from the ground surface to 100 m below sea level. The mesh was tested based on the Delaunay criterion in order to avoid numerical problems. The flow time step, Δt, was set at a fixed number of 5 days. The convergence criterion for the groundwater flow equation was 0.001 m.

2.3.2. Model scenarios relevant to climate changes

The objective of this modeling study was to investigate how the changing climate affects the groundwater system and the process of soil gleyization in this low-lying alluvial-lacustrine plain by 2050. Therefore, to reasonably forecast the effects, we considered ongoing global climate change (with different regional climate models) and their consequences for future meteorological and hydrological conditions such as precipitation and surface water level.

Popular climate models have generated different scenarios of future water level and river discharge at the catchment scale in the PLB (Guo et al., 2008; Ye et al., 2011; Sun et al., 2012). However, we took the results by Ye et al. (2011) and Li et al (2016) because they have been devoted to studying the evolution of the river-lake relationship influenced by climate changes and have accumulated substantial local information for the PLB for > 10 years. Furthermore, they have established a regression model to calculate the change of surface water level, a key input for groundwater modeling, in response to inflow variations under different climate scenarios. These climate scenarios of A2 (high carbon dioxide emission), A1B (mid-range carbon dioxide emission), and B1 (low carbon dioxide emission), were based on the global circulation model ECHAM5 (IPCC, 2007). For the PLB, prediction for long-term average changes in precipitation and hydrologic conditions have been made with the large-scale, distributed hydrological model, WATLAC (Zhang and Werner, 2009), based on these three carbon dioxide emission scenarios (Fig. 7) (Ye et al., 2011). The results indicated that changes in the annual cycle of precipitation were mostly projected to increase in March–October and decrease in November–February. Moreover, the total inflows from the catchment will increase in the wet period and decrease in the dry period under future climate conditions, resulting in possible changes in water levels for the wet (0.1–1.34 m) and dry (−0.32 to −1.31 m) seasons in the river-lake system. The changing meteorological and hydrological data (2016–2050) predicted by Ye et al. (2011) was applied as future boundary conditions in our modeling to forecast the future hydrogeological system response and, in turn, the process of soil gleyization using a well-calibrated groundwater model.

3. Results and discussion

3.1. Relationship between groundwater depth and gleyization

3.1.1. In-situ sampling results

The main indicators of ARS, Fe^{2+}, and Eh of 120 soil samples collected at the depths of 0–30 cm and 30–60 cm at the 5 sampling sites (S-01–S-05) (Fig. 2) were analyzed in the soil testing laboratory. The ARS and Fe^{2+} contents were plotted in a base 10 logarithmic coordinate system as shown in Fig. 8(a). A linearly increasing correlation between

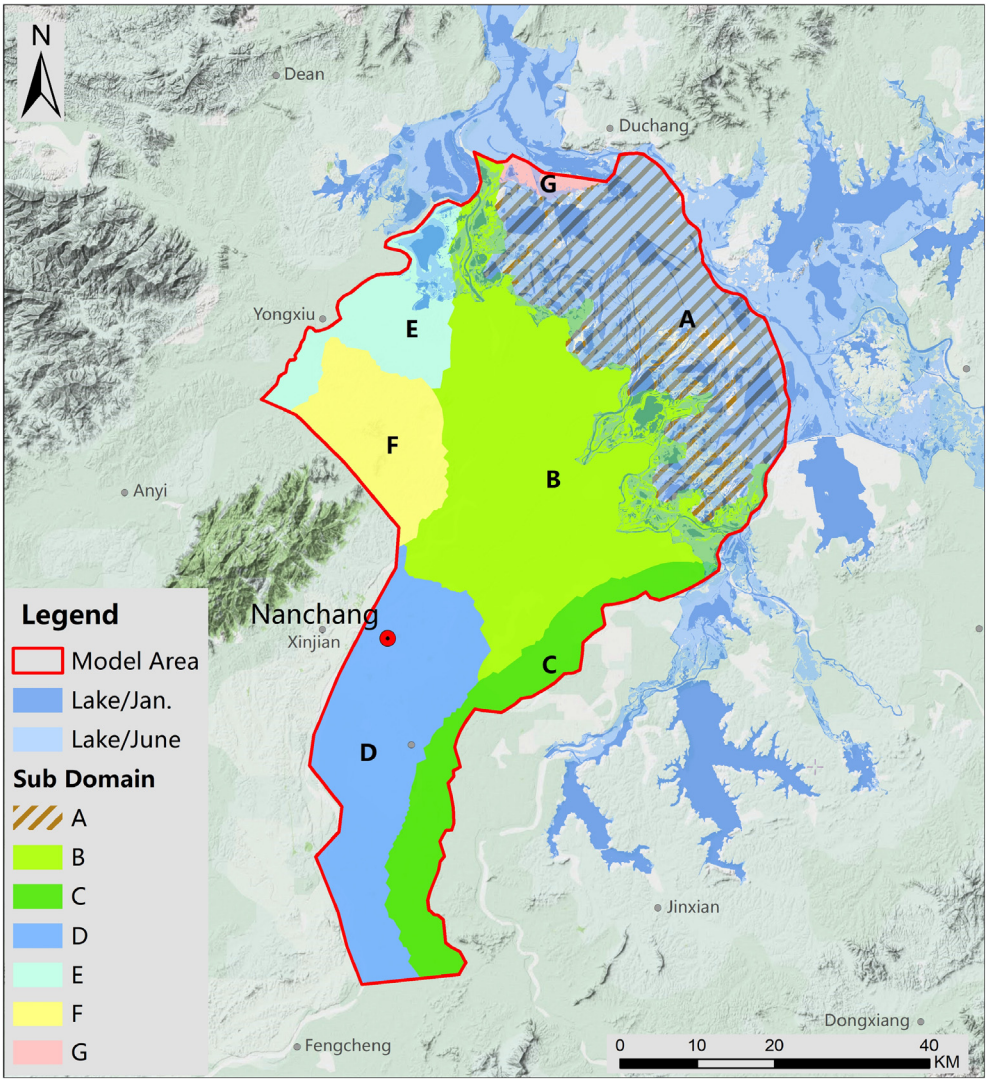

Fig. 6. Parameter zonation of net recharge rate in Layer 1, and horizontal hydraulic conductivity, specific yield, specific storage in Layer 1 and Layer 2.

ARS and Fe^{2+} was obtained indicating that Fe^{2+} ions made up the major components (about 89%) of acting reducing substances, leaving 11% of the organic compounds. The ARS content and Eh was plotted in a linear coordinate system as shown in Fig. 8(b). The Eh decreased as the ARS increased, showing a descending relationship. The Eh represents the degree of reduction in the soil, mainly because the quantity of the reduced material determines the measured mixed potential at the platinum electrode. However, the quantity of ARS in reduced soil determines the intensity of damage to plant growth. Taking the S-01 series with a small variation of the Eh value as an example, the soil fertility will decrease as the ARS content increases because of different GDs in different seasons.

Based on the test results, a statistical analysis was conducted to determine the relationship between GD and the gradation of gleyization. Statistical results of GD corresponding to different intervals of ARS, Fe^{2+}, and Eh values (Table 1) were visualized in a box and whisker plot (Fig. 9). The maximum, minimum, and average values, along with the interquartile range of GD, were also tabulated for each interval of index characterizing gleyization (Table 2). When ARS > 3.0 cmolc/kg, Fe^{2+} > 2.5 cmolc/kg, and Eh < 100 mV (defined as highly gleyed soil), the variation ranges of GD were all between 0 and 9 cm. When 0.7 < ARS < 3.0 cmolc/kg, 0.5 < Fe^{2+} < 2.5 cmolc/kg, and 100 < Eh < 300 mV (defined as medium gleyed soil), the variation ranges of GD are between 15 and 46 cm, 17 and 47 cm, and 16 and 49 cm, respectively. When 0.1 < ARS < 0.7 cmolc/kg, 0.05 < Fe^{2+} < 0.5 cmolc/kg, and 300 < Eh < 500 mV (defined as slightly gleyed soil), the variation ranges of GD were between 38 and 83 cm, 38 and 85 cm, and 37 and 84 cm, respectively. When ARS < 0.1 cmolc/kg, Fe^{2+} < 0.05 cmolc/kg, and Eh > 500 mV (defined as ungleyed soil), the variation ranges of GD were between80 and 100 cm, 80 and 99 cm, and 78 and 102 cm, respectively. Therefore, from the viewpoint of field testing, the four types of gleyed soil (highly gleyed, medium gleyed, slightly gleyed, and ungleyed), are related to the GD of < 10 cm, 10–50 cm, 50–85 cm, > 85 cm in GRD area, respectively as shown in Table 3.

3.1.2. *Laboratory experiment results*

The experimental results (Fig. 10) show that under the same experimental conditions of temperature, precipitation, and basic physical properties of soil, that as Eh values increased the ARS and Fe^{2+} content decreased with the lowing of the water table. The degree of soil gleyization was positively associated with the groundwater level. The change of gleyed indexes was quite prominent in the top soil layer (L1) as the inundated condition was greatly influenced by the groundwater fluctuations. However, the variability of indexes of soil gleyization in deep soil layers (L3 and L4) were smaller, especially when the groundwater level fluctuated at the depth of 0–40 cm. The laboratory experiment results indicates that the flooded conditions have a great

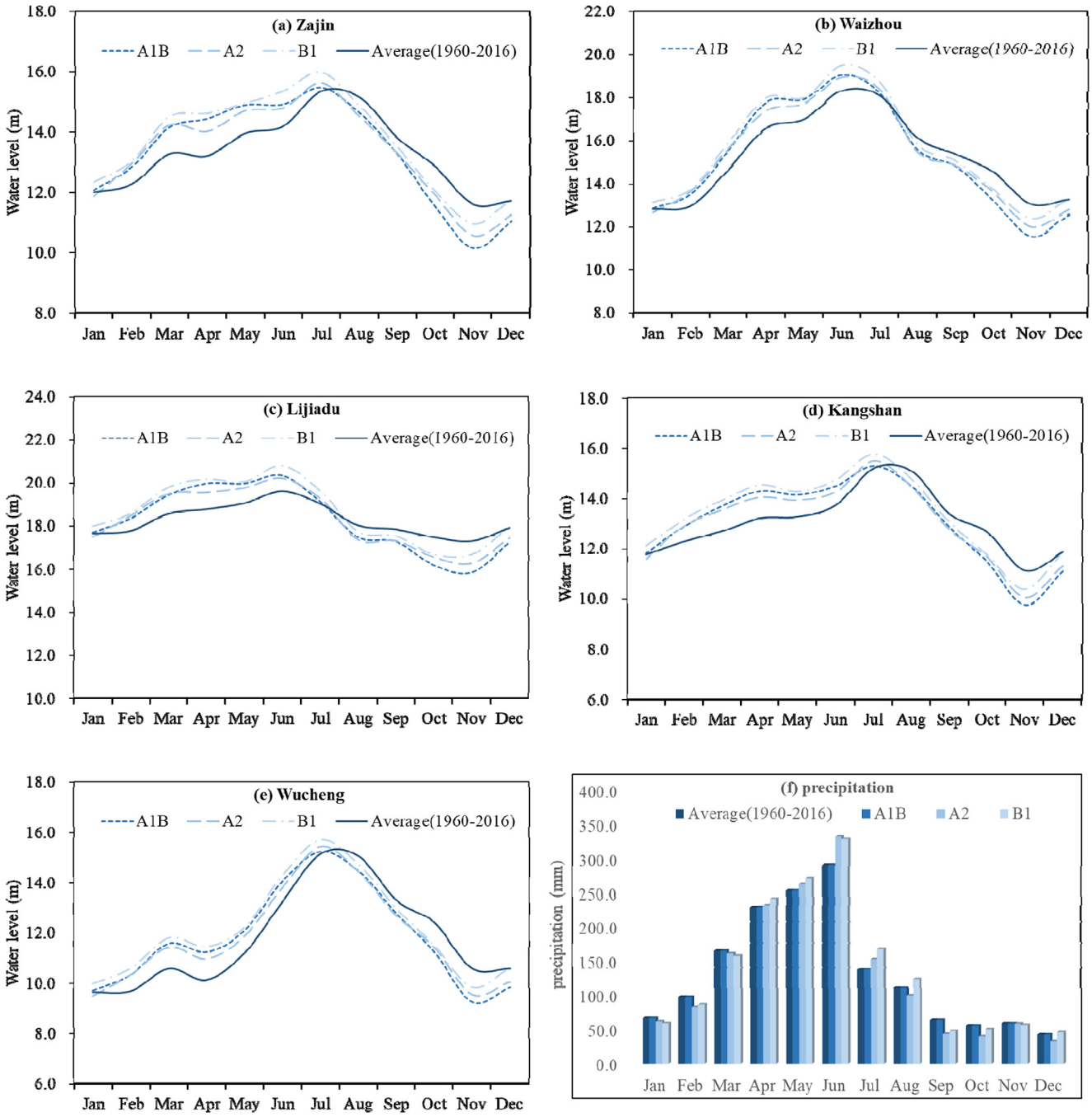

Fig. 7. Long-term monthly average surface water level at five gauging stations (a)–(f) and precipitation (g) for 2016–2050 compared to the historical average data for 1956–2016.

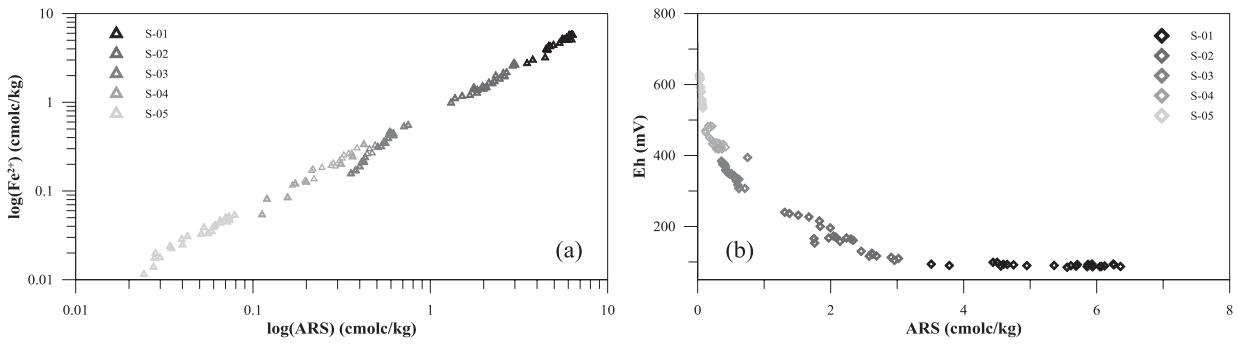

Fig. 8. Relationship between (a) ARS and Fe^{2+}, (b) ARS and Eh value in sampling soil.

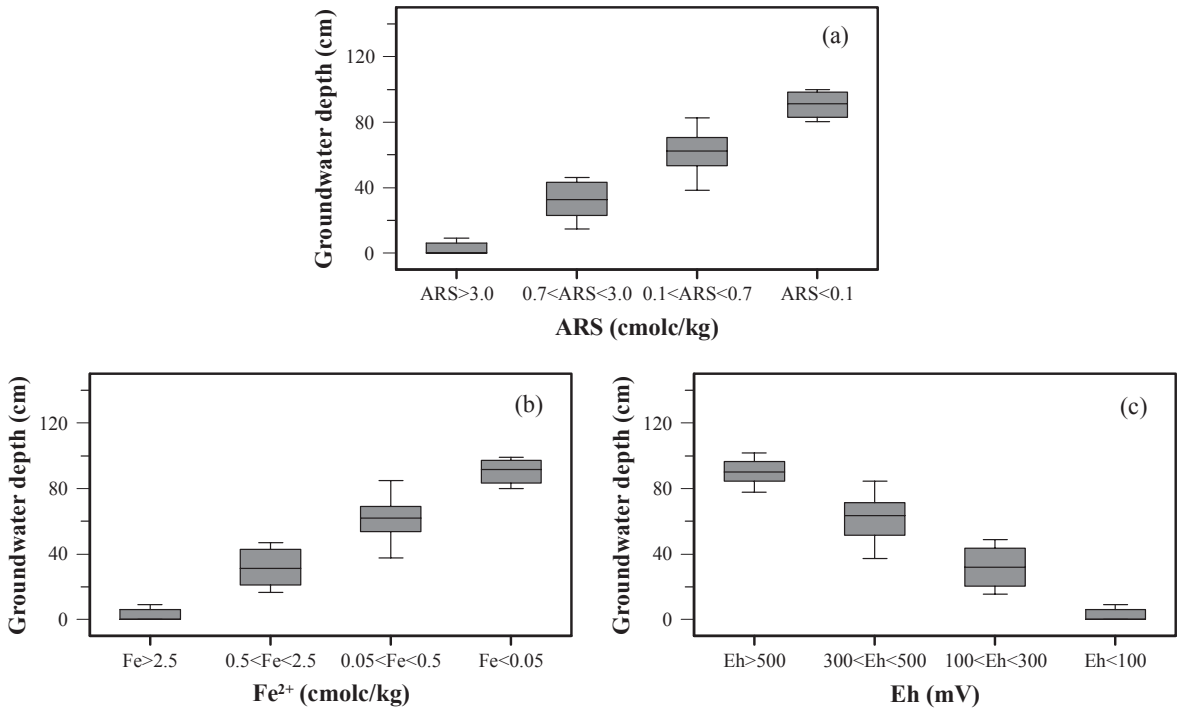

Fig. 9. Box and whisker plot showing ranges in groundwater depths corresponding to different intervals of (a) ASR, (b) Fe^{2+}, and (c) Eh.

influence on indexes of soil gleyization, the saturated soil layers had larger ARS and Fe^{2+} contents and smaller Eh values than in layers under unsaturated conditions. With GD = 0 cm, the average gleyization indexes (represented as (ARS, Fe^{2+}, Eh) from here on) of the 4 soil layers were (4.4 cmolc/kg, 3.7 cmolc/kg, 90.1 mV), belonging to the highly gleyed soil. With GD = 20 cm, soil layer L1 with average (2.5 cmolc/kg, 1.9 cmolc/kg, 167.6 mV), belonging to the medium gleyed soil, and layers L2– L4, with average (3.7 cmolc/kg, 3.1 cmolc/kg, 96.5 mV) belonging to the highly gleyed soil. With GD = 40 cm, soil layers L1–L2 with average (1.2 cmolc/kg, 0.8 cmolc/kg, 236.5 mV), belonging to the medium gleyed soil, and layers L3–L4, with average (3.0 cmolc/kg, 2.7 cmolc/kg, 115.3 mV) belonging to the highly gleyed soil. With GD = 60 cm, soil layers L1– L4 with average (1.3 cmolc/kg, 0.9 cmolc/kg, 385.9 mV), belonging to the medium—slightly gleyed soil. With GD = 80 cm, soil layers L1–L4 with average (0.13 cmolc/kg, 0.07 cmolc/kg, 507.7 mV), belonging to the slightly—ungleyed soil. The results of the laboratory experiment investigation of gleyed indexes verifies the relationship between GD and gradation of soil gleyization identified in the in-situ sampling.

In this study, in-situ sampling and testing and laboratory experiments have their respective limitations. The testing results from in-situ sampling at different sampling sites ignored the effects of soil properties on soil gleyization. The laboratory experiments used the same undisturbed soil samples, but each soil saturated condition was established under steady state conditions with a constant water table. In reality, soil gleyization will be time dependent due to the fluctuations of the water table. These limitations of the in-situ sampling and testing and laboratory experiments may affect model predictions about future soil gleyization at smaller local scale. However, given the focus of this study is on the much larger regional scale, these limitations are not expected to have a strong influence on the predicted patterns of future soil gleyization. Notwithstanding these limitations, the relationship between GD and gradation of soil gleyization obtained with these two measurement methods was cross verified. The relationship indicated that the groundwater depth is an indirect indicator for classifying soil gleyization, in which the regional variable of GD can be predicted by groundwater modelling.

Table 3
Groundwater depth for distinguishing soil types with different graduation of gleyization.

Gleyization type	ARS (cmolc/kg)	Fe^{2+} (cmolc/kg)	Eh (mV)	GD (cm)
Highly gleyed	> 3.0	> 2.5	< 100	< 10
Medium gleyed	0.7–3.0	0.5–2.5	100–300	10–50
Slightly gleyed	0.1–0.7	0.05–0.5	300–500	50–85
Ungleyed	< 0.1	< 0.05	> 500	> 85

3.2. Model results and discussion

3.2.1. Model calibration and validation

The numerical model was calibrated and validated under transient

Table 2
Statistics of groundwater depths corresponding to different intervals of ARS, Fe^{2+}, and Eh.

GD (cm)	Intervals of ARS (cmolc/kg)				Intervals of Fe^{2+} (cmolc/kg)				Intervals of Eh (mV)			
	> 3.0	0.7–3.0	0.1–0.7	< 0.1	> 2.5	0.5–2.5	0.05–0.5	< 0.05	> 500	300–500	100–300	< 100
Minimum	0	15	38	80	0	17	38	80	78	37	16	0
Maximum	9	46	83	100	9	47	85	99	102	84	49	9
Average	2	31	61	90	2	31	61	90	90	61	32	2
25th percentile	0	23	53	83	0	21	54	83	85	52	20	0
75th percentile	6	43	71	98	6	43	69	97	97	71	44	6

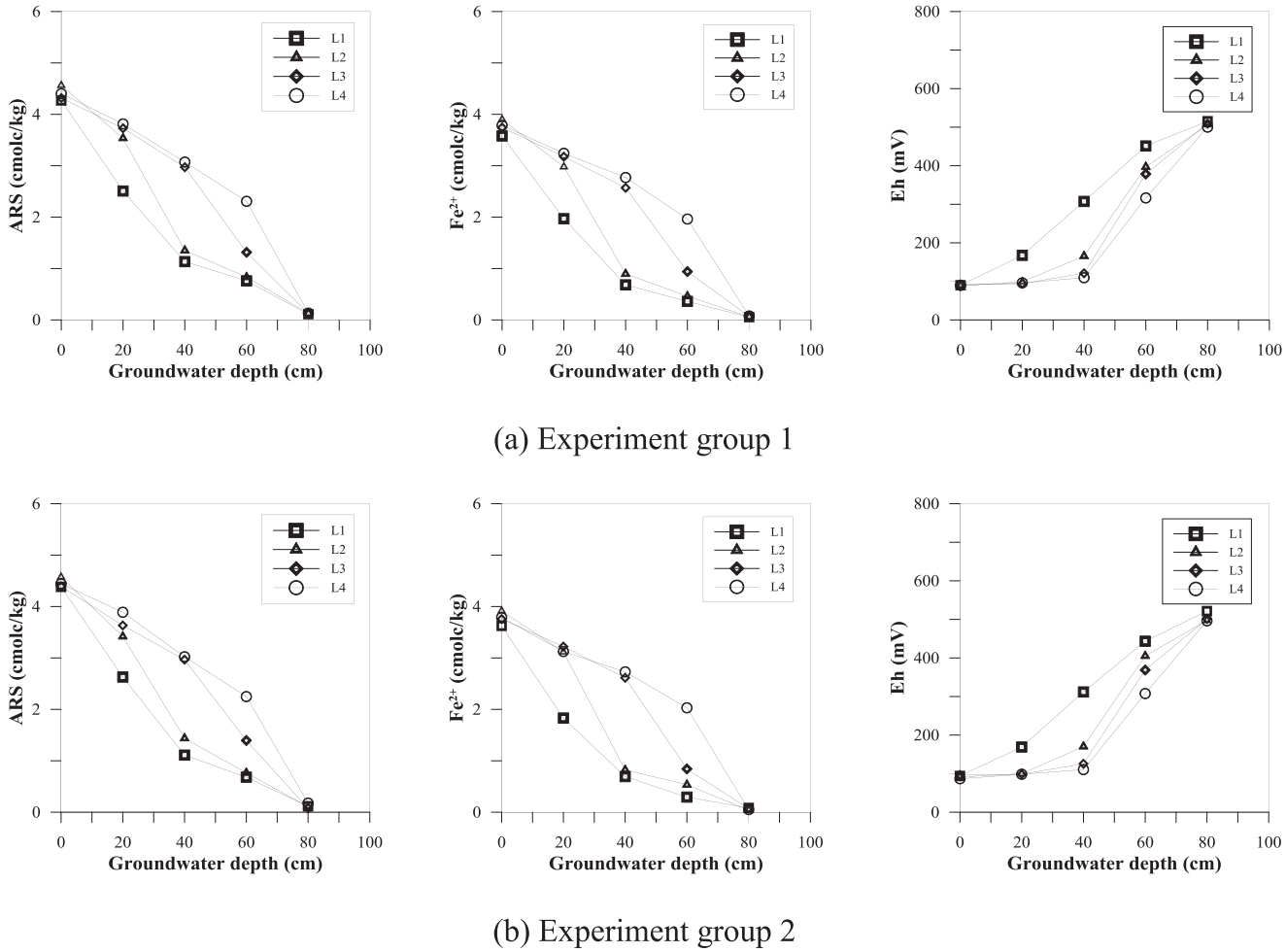

Fig. 10. Variation of the gleyization indexes of four layers (L1, L2, L3, and L4) in the soil column with different depths to water table.

conditions by trial and error procedure. Firstly, a steady-state model generated the initial conditions for the transient model. Secondly, the measured groundwater heads of 19 observation wells from 1/1/1986 to 31/12/1986 were chosen as transient calibration targets. Calibration was performed by a trial and error procedure until a reasonable agreement was achieved between the simulated and measured groundwater levels (Fig. 11). Thirdly, the calibrated model was validated based on whether it matched the set of field data of 11 observation wells from 1/1/2010 to 31/12/2010, which were independent of the data used for model validation.

We used 456 head measurements (19 wells × 24 transient data per well) in 1986 for model calibration, which were distributed through all aquifers. The median of the difference between the calculated minus measured groundwater heads was 0.12 m. The median of the absolute difference was 0.43 m with a standard deviation of 0.41 m. After model calibration, we selected 264 transient observed data in 2010 for model validation. The median of the difference and absolute difference between transient series of simulated and observed values are 0.23 m and 0.45 m with a standard deviation of 0.33 m. Scatter diagrams of simulated groundwater level against the observed value and the histogram of differences between simulated and observed groundwater head after transient calibration and validation are shown in Fig. 11. We believe these differences represent good calibration and validation results relative to maximum and minimum ground surface elevation in this area, though calibration of heads of the model domain was difficult in the cone of depression in Nanchang City where significant centralized groundwater extraction occurred.

In addition, the calculated GD and corresponding soil gleyization type of the 5 soil sampling sites (S-01–S-05) (see Fig. 2) were compared with measured ones (Table 4). The calculated gleyization type was determined by the statistical relation to GD as described above in Table 3. The calculated type for the sampling sites were consistent with the results measured in-situ, except for minor difference in S-03 and S-04 sites. For S-03 site, the measured gleyization type was defined as medium-slightly gleyed compared to the calculated type of medium gleyed. In flat and dry seasons, the soil in S-03 site was slightly gleyed as the measured average GD was 53.7 cm (50 < GD < 85 cm), while in wet season, the soil became medium gleyed as the water table rose to the minimum GD of 38.5 cm (10 < GD < 50 cm). The overall calibration results indicate that the applied groundwater modeling can serve as an indirect tool for evaluating the degree of soil gleyization at regional scale. Therefore, the net recharge rate of the top layer and the horizontal hydraulic conductivity of the principal aquifers, that are improved (i.e., optimized) after model calibration and validation, were implemented in the model assessment and prediction (Table 5).

3.2.2. *Model climate scenario assessment*

In response to the changes of future long-term average meteorological and hydrological conditions, the groundwater flow will also change according to changes in the corresponding boundary conditions and source/sinks. The anticipated long-term average surface water level and precipitation were set as specified head boundary conditions and repeated annually in the transient predictive model. The constant head boundaries of Poyang Lake and the three perimeter rivers (Ganjiang River, Xiu River, and Fu River) were set at the predicted values, and the parameter of net recharge rate was scaled up or down corresponding to

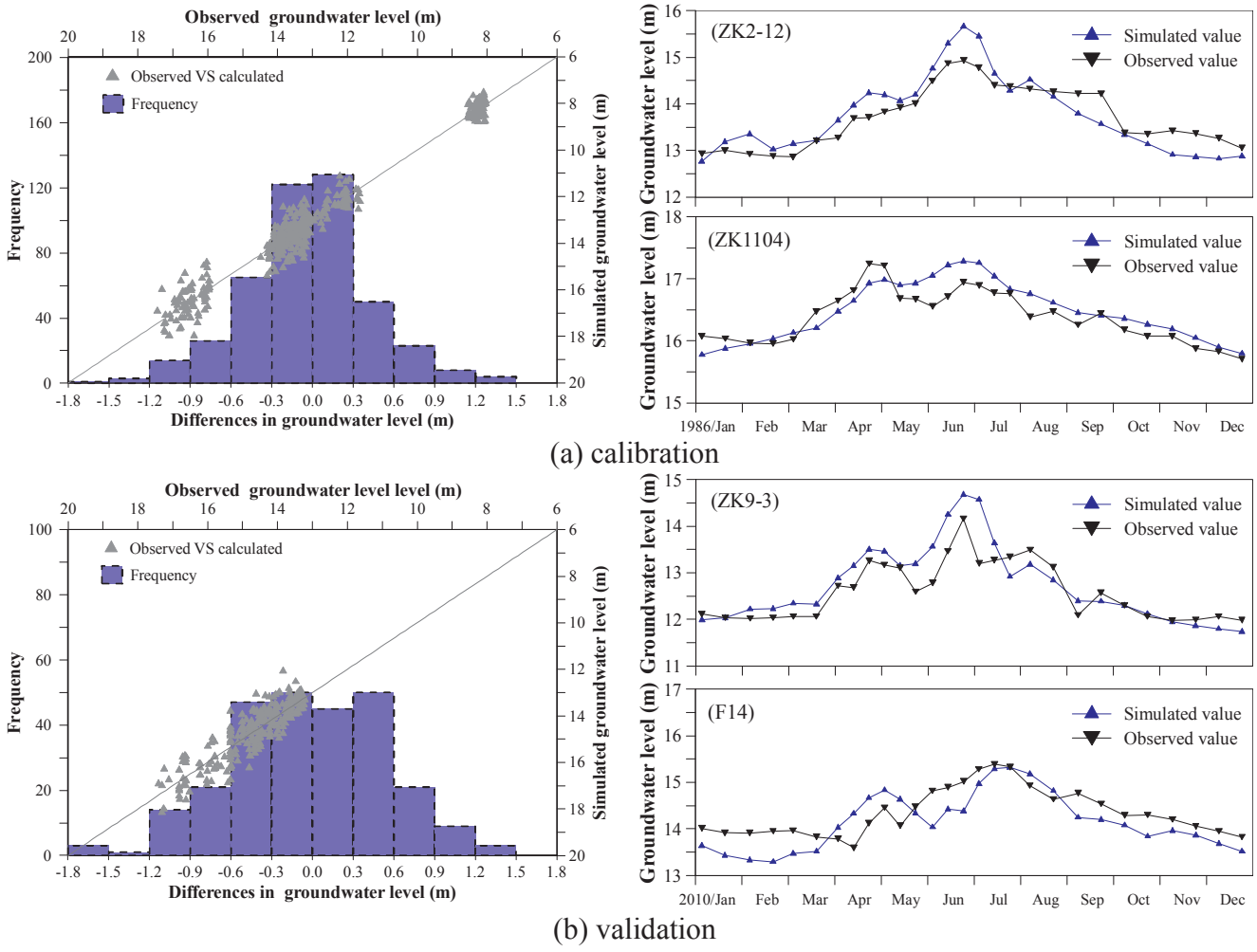

Fig. 11. Scatter diagrams of simulated groundwater level against the observed value and histogram of differences between simulated and observed groundwater level in meters for transient (a) model calibration and (b) model validation.

Table 4
Comparison of groundwater depth and corresponding gleyization type between calculated and measured values.

Soil sample	Average GD (cm)		Minimum GD (cm)		Gleyization type	
	Calculated	Measured	Calculated	Measured	Calculated	Measured
S-01	8.3	1.9	0.0	0.0	Highly	Highly
S-02	43.9	31.3	26.3	14.8	Medium	Medium
S-03	45.1	53.7	30.9	38.5	Medium	Medium-silghtly
S-04	89.1	71.0	76.4	61.0	Slightly-ungleyed	Slightly
S-05	110.3	90.4	95.9	80.3	Ungleyed	Ungleyed

Table 5
The hydrogeological parameters used in the GRD groundwater flow model after calibration.

Parameters	Layer A1		Layer A2		Layer A3	
	Nos. of Zone	Range	Nos. of Zone	Range	Nos. of Zone	Range
Horizontal hydraulic conductivity, K_h (m/d)	7	0.005–5.0	7	0.05–135.0	1	0.001
vertical anisotropy ratio, K_h/K_v	1	0.2	1	1.0	1	1.0
Net recharge rate, R (mm/year)	7	0.16–29.8	0	–	0	–
Specific yield S_y	7	0.1–0.35	–	–	–	–
Specific storage, S_S (/m)	–	–	7	0.0001–0.001	1	0.0001

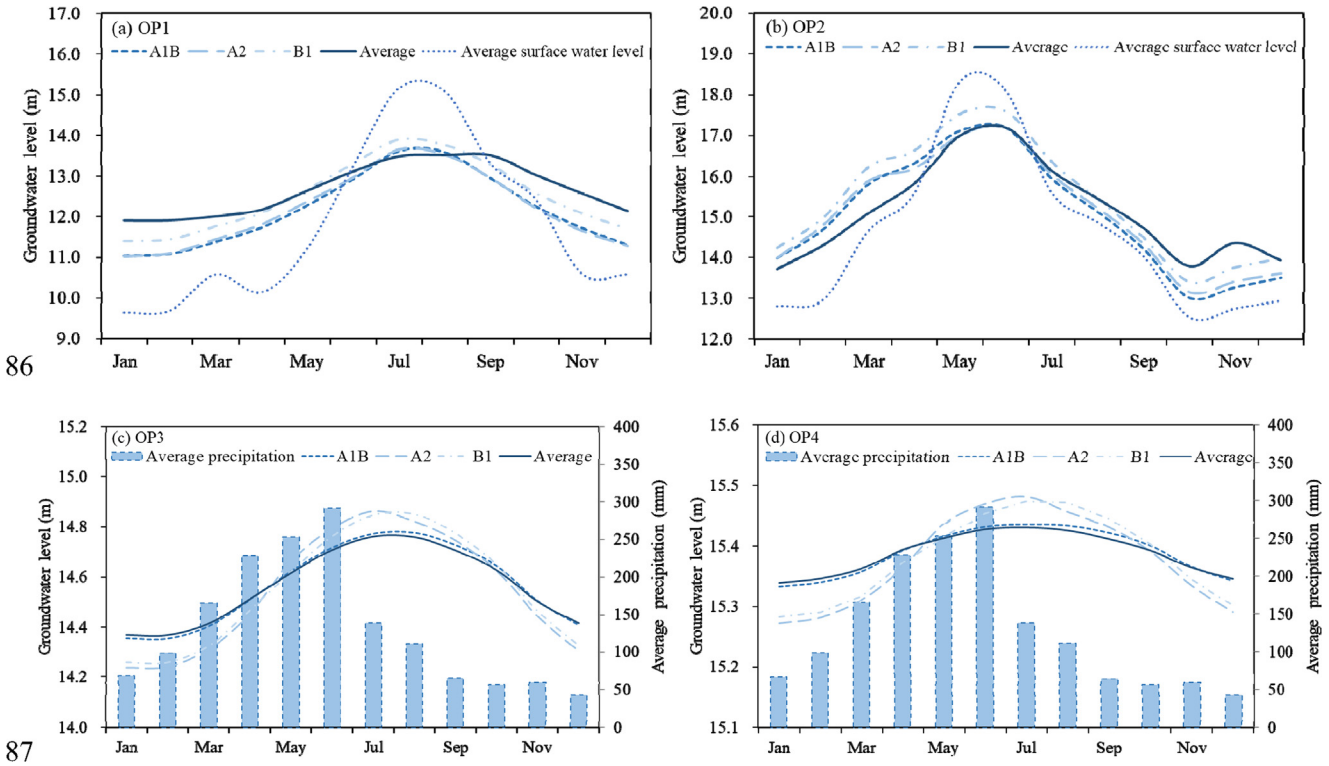

Fig. 12. The predicted long-term average groundwater levels with three climate scenarios for 2016–2050 in four observation points compared with the groundwater level predicted with annual average condition, (a) for OP1, (b) for OP2, (c) for OP3, and (d) for OP4.

an increased or decreased ratio of precipitation for all climate scenarios. For example, in the Scenario A2, the constant head boundaries of the Poyang Lake and three perimeter rivers were set with an increased surface water level between 0.29 m and 0.65 m from February to July and a reduced level between 0.15 m and 1.04 m from August to January. Meanwhile, the recharge rate was assigned an increased value between 1.6% and 14.3% from April to July and a reduced value between 0.4% and 15.2% from August to March. The hydraulic heads resulting from the calibrated three-dimensional model were set as the initial condition for the transient prediction model while all the other input hydrogeological parameters remained unchanged. The model was run for 34 years (2016–2050) in transient conditions.

The long-term average groundwater levels at four observation points (OP1–OP4) predicted using three climate scenarios were compared with results from the model based on annual averages, as shown in Fig. 12. OP1 and OP2 were located close to the bank of Poyang Lake and Ganjiang River, while OP3 and OP4 were placed in the middle part of the study region between the watercourses, respectively. From the prediction results at OP1 and OP2 sites (Fig. 12a, b), the groundwater levels of three climate scenarios were lower than the levels of annual average conditions because of the reduction in surface water levels caused by climate changes in the dry season after September. The period of the maximum decline was the driest period between November and December and the maximum decline of groundwater level was 1.1 m for the Scenario A1B. After March, the river level affected by climate change was higher than the average data and the groundwater level gradually increased. By May, the groundwater heads recovered to the annual average state and gradually exceeded the predicted results for the average scenario in the lakeside area. The period of the maximum increase in groundwater level was the wettest period between June and July corresponding to a maximum increase of 1.2 m for the Scenario B1. We also compared the predicted long-term average groundwater level with the average surface water levels at a nearby gauging station, as shown in Fig. 12a, b. The results highlight that both the surface water level and groundwater level showed obvious annual variation and the trends in their change were largely consistent, indicating that a close hydraulic connection exists between the main watercourses and the alluvial aquifer. Based on the relative elevations of stream stage and the groundwater head adjacent to the stream, groundwater mainly discharged to surface water bodies at the sites close to the lake and rivers, while surface water recharged groundwater between June and August when surface water level rapidly increases with the increasing of inflow from upstream areas.

In addition, the prediction results in OP3 and OP4 sites (Fig. 12c, d) had yearly groundwater level fluctuation ranges of 0.6 and 0.3 m, respectively, which are much smaller than the variation range of level in the nearest river. However, the trend of changing groundwater level was consistent with the variation of precipitation and the increase or decline in groundwater level was coherent with changes in precipitation under the three climate scenarios compared with the annual average conditions. The decline in groundwater levels of the Scenarios A2 and B1 was higher than the decreasing scope of A1B and average conditions due to the decrease in precipitation caused by climate changes in the dry season after September. The period of the maximum decline was the dry period between December and January and the maximum decline of groundwater level was 0.13 m for the Scenario A2. After April, the precipitation affected by the Scenarios A2 and B1 was higher than the A1B and average data and the groundwater level was at a corresponding higher level. The period of the maximum increase in groundwater level was the wet period between June and July with corresponding maximum increase of 0.1 m for the Scenario B1. The prediction results for OP3 and OP4 sites indicate that in the middle region between river courses, the groundwater level was relatively affected by changing precipitation and had a much weeker hydraulic connection with surface water.

The groundwater level in the aquifer increased from March and reached the peak in late June to early August, then decreased from September and hit the lowest point in late December to January. The highest groundwater heads of the prediction models, corresponding to peaks in groundwater head fluctuations, for the three climate scenarios

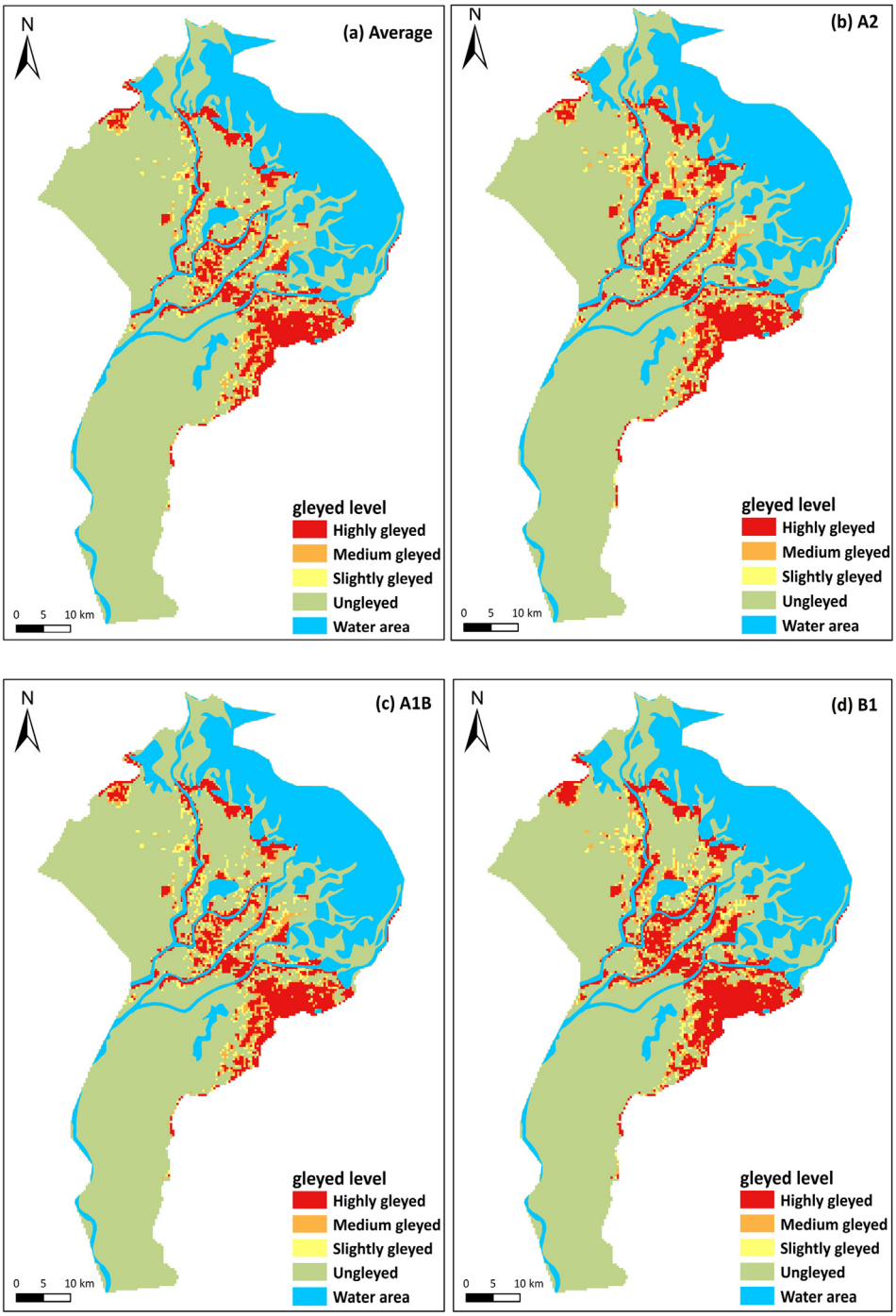

Fig. 13. Potential soil gleyization estimated by groundwater model for (a) annually average condition and three climate scenarios (b) A2, (c) A1B, and (d) B1.

and annual average conditions (Fig. S1) were selected to evaluate the greatest influence level of groundwater saturation conditions on soil gleyization. Based on the statistical relationship between GD and the gradation of soil gleyization discussed in Table 3 of Section 3.1.1, the potential soil gleyization estimated with the groundwater model for all four scenarios is shown in Fig. 13. The alluvial area among the three branches of the Ganjiang River and the area of the lower reaches of the Fu River are the low-lying region in the GRD, causing poor drainage condition with water-logged conditions in impervious paddy soils that resulted in highly gleyed irrigation farmland in the wettest season (from June to August). During this period, when the early-season rice is at the reproductive phases of heading, grain filling and maturity, and the late-season rice is at the vegetative stages of seeding development and tillering in PLB, the hydrogeological environment will accelerate soil gleyization and lead to the reduction of oxygen and the generation of significant reductive substances, thereby widely and negatively affecting rice production (Liu et al., 2015). For the Scenario B1, highly and medium gleyed areas will increase substantially near the three branches of the Ganjiang River and the lower reach of the Fu River. This is because of the maximum increase of surface water level and expansion of the medium-slightly gleyed area in the middle region between river courses due to the maximum increase of precipitation in June–-July season. For the Scenario A1B, the highly-medium gleyed area will increase slightly along the three branches of Ganjiang River due to a slight increase of surface water level in the wettest season. In contrast, for the Scenario A2, medium-slightly gleyed area will expand

Table 6
The spatial area of gleyed region that will be suffered from the change of groundwater depth between 2016 and 2050.

Climate scenarios	Gleyed area (km^2)			
	Highly gleyed	Medium gleyed	Slightly gleyed	Total area
Annually average	372.0	74.4	111.6	558.0
A2	379.4	81.8	120.5	581.7
A1B	375.7	75.8	113.8	565.3
B1	401.7	82.5	122.7	606.9

considerably in the middle region due to the large increase of precipitation in the wettest season. Therefore, compared with annual conditions, the Scenario A1B will result in comparatively small impacts on soil gleyization; the Scenario A2 will increase 16.3 km^2 of medium-slightly gleyed area; and, the Scenario B1 will exert an influence of > 48.9 km^2 of total gleyed area, including 29.7 km^2 of highly gleyed area and 19.2 km^2 of medium-slightly gleyed area (Table 6). To summarize, the predicted changes of the surface water level and precipitation suggest higher potential severity in the expansion of soil gleyization in the wettest season under the climate scenario B1.

Although the underlying science for climate change adaption and the selection of climate scenarios are highly uncertain, the variation tendency of groundwater level in the model output was consistent with that of surface water level and precipitation. If more accurate and reliable climate scenarios are obtained in the future relying on different types of newly available data, the corresponding groundwater level should achieve annual change trends that are consistent with the trends in meteorological and hydrological conditions. Thus, more accurate impacts on soil gleyization could be predicted by the three-dimensional groundwater model proposed in this study.

4. Conclusions

In this study, the alluvial-lacustrine low-lying area of the Ganjiang River Delta (GRD) in the western Poyang Lake Basin, already endangered by soil gleyization, was selected to investigate the effect of future climate change on the formation of gleyed farmland. Soil sampling analysis and column experiments were implemented to explore the formative mechanism of soil gleyization at a regional scale and to establish the statistical relationship between groundwater depth (GD) and the gradation of soil gleyization in the GRD. A three-dimensional groundwater flow model was developed and calibrated to implement four model scenarios to forecast the impacts of the projected annual average condition and three climate scenarios (A2, A1B, and B1) on the average changes of groundwater level and the potential maximum severity of soil gleyization from 2016 to 2050.

Results show that the GRD with depressed land surfaces, waterlogged conditions, and impervious soil medium possessed the hydrological and hydrogeological conditions favorable for soil gleyization. The quantity of the active reducing substance, ferrous iron content, and redox potential were the three principal indexes for identification of the types of soil gleyization, each index contributing to the consequence of groundwater saturation conditions in terms of GD. The statistical relationship between GD and gradation of soil gleyization was established by comparing results of field soil sampling analysis and laboratory experimental results. It was shown that four types of gleyed soil (highly gleyed, medium gleyed, slightly gleyed, and ungleyed) were related to the GDs of < 10, 10–50, 50–85, > 85 cm, respectively in the GRD area. Scenario modeling results of the long-term average groundwater level (2016–2050) showed annual change trends consistent with the meteorological and hydrological conditions. In the riverside area, a close hydraulic connection was present between the main watercourses and the alluvial aquifer, whereas in the middle region between rivers, the groundwater was relatively affected by changes in precipitation and had much weeker hydraulic connection with surface water. For the Scenario B1 (low carbon dioxide emission), the groundwater level was shown to increase in the riverside area of three branches of the Ganjiang River and lower reaches of the Fu River due to the increase of surface water level. It was shown to increase in the middle region between the river courses under the increase of precipitation, and accordingly gleyization of these low-lying regions would intensify. Compared with the annual conditions, highly gleyed areas increased by 29.7 km^2 (mainly in the riverside area) and the medium-slightly gleyed areas increased by 19.2 km^2 in the middle region under the Scenario B1. The climate scenario B1 would very likely exacerbate the soil gleyization already experienced by these reclaimed farmlands.

This study has contributed to identifying the impacts of GD on soil gleyization at the regional scale. It has established a three-dimensional groundwater flow model in the GRD shallow aquifer to demonstrate the major impact of climate changes on soil gleyization. It is of great importance to land resource managers to plan choices and implementation of engineering measures to mitigate soil gleyization of low-lying and water-logged reclaimed farmland. Future research should focus on the implementation of mitigation initiatives such as ditch drainage network systems, and ridge agriculture in the simulation-optimization framework to achieve optimal agricultural management measures.

Acknowledgements

This work was partially supported by the National Key R&D Program of China (No. 2016YFC0402800), the National Natural Science Foundation of China (Nos. 41772254, 41502226, and 41402198), and the Fundamental Research Funds for the Central Universities (No. 2018B18714). We are grateful to Jiangxi Institute of Survey and Design, who provides the detailed hydrogeological data of PLB for establishing three-dimensional groundwater flow model. Yun Yang gratefully acknowledges financial support from China Scholarship Council (CSC No. 201706715023) during the visit to National Centre for Groundwater Research and Training (NCGRT), Australia. Behzad Ataie-Ashtiani and Craig T. Simmons acknowledge support from the National Centre for Groundwater Research and Training, Australia. We are grateful to the Editor and two anonymous reviewers whose invaluable suggestions have led to significant improvement in this manuscript.

Appendix A. Supplementary data

Supplementary data to this article can be found online at https://doi.org/10.1016/j.jhydrol.2018.11.006.

References

Balbarini, N., Boon, W.M., Nicolajsen, E., Nordbotten, J.M., Bjerg, P.L., Binning, P.J., 2017. A 3-D numerical model of the influence of meanders on groundwater discharge to a gaining stream in an unconfined sandy aquifer. J. Hydrol. 552, 168–181.

Brammer, H., Brinkman, R., 1977. Surface-water gley soils in Bangladesh: Environment, landforms and soil morphology. Geoderma 17, 91–109.

Brown, I., 2017. Climate change and soil wetness limitations for agriculture: Spatial risk assessment framework with application to Scotland. Geoderma 285, 173–184.

Burbaum, B,, Fleige, H., Horn, R., 2016. Soil of the year 2016: Groundwater soil (Gley). Ministry of Energy, Agriculture, the Environment and Rural Areas of Schleswig-Holstein.

Clagnan, E., Thornton, S.F., Rolfe, S.A., Tuohy, P., Peyton, D., Wells, N.S., Fenton, O., 2018. Influence of artificial drainage system design on the nitrogen attenuation potential of gley soils: evidence from hydrochemical and isotope studies under field-scale conditions. J. Environ. Manage. 206, 1028–1038.

DEFRA Impact of climate change on soil functions 2005 Final Project Report Research and Development, London, UK.

Diersch, H.J.G., 2014. FEFLOW: finite element modeling of flow, mass and heat transport in porous and fractured media. P.996 URL: https://doi.org/10.1007/978-3-642-38739-5.

Epting, J., Huggenberger, P., Radny, D., Hammes, F., Hollender, J., Page, R.M., Weber, S., Banninger, D., Auckenthaler, A., 2018. Spatiotemporal scales of river-groundwater interaction-The role of local interaction processes and regional groundwater regimes. Sci. Total Environ. 618, 1224–1243.

Fiedler, S., Vepraskas, M.J., Richardson, J.L., 2007. Soil redox potential: importance, field measurements, and observations. Adv. Agron. 94, 1–57.
Guo, Y.Z., Chen, L.S., 2008. Investigation Report on Groundwater Resources in Poyang Lake Basin. Jiangxi Province, Jiangxi Geology & Mineral Exploration Bureau Report No 0900324852.
Guo, H., Hu, Q., Jiang, T., 2008. Annual and seasonal streamflow responses to climate and land-cover changes in the Poyang Lake Basin. J. Hydrol. 355, 106–122.
Havril, T., Tóth, A., Molson, J.W., Galsa, A., Mádl-Szőnyi, J., 2017. Impacts of predicted climate change on groundwater flow systems: can wetlands disappear due to recharge reduction? J. Hydrol. https://doi.org/10.1016/j.jhydrol.2017.09.020.
IPCC, 2007. Climate Change 2007: The Physical Science Basis. Cambridge University Press, Cambridge/New York.
Jiangxi Institute of Red Soil, 1987. Investigation of Soil Resources in Poyang Lake Region. Poyang Lake Comprehensive Scientific Investigation Team Report.
Karmakar, R., Das, I., Dutta, D., Rakshit, A., 2016. Potential effects of climate change on soil properties: a review. Sci. Int. 4, 51–73.
Lai, X., Liang, Q., Jiang, J., Huang, Q., 2014. Impoundment effects of the three-gorges-dam on flow regimes in two china's largest freshwater lakes. Water Resour. Manage. 28 (14), 5111–5124.
Lai, Q.W., Liu, X., Huang, Q.H., 1989. The genesis of paddy soil gleyization and its amendment strategy in Poyang lake region. Sci. Agric. Sin. 22 (4), 65–74.
Li, D.M., Yu, X.C., Liu, K.L., Ye, H.C., Xu, X.L., Zhou, L.J., Hu, H.W., Huang, Q.H., 2015. Remediation effect of the combination of ditching drainage and agronomic managements on gleyed paddy field in Poyang Lake Region China. J. Plant Nutr. Fertilizer 21 (3), 684–693.
Li, Y., Wei, X.J., Gao, B.Z., Wu, A.G., Wan, Z.B., 2008. Geological Map of Jiangxi Province (1:500000). Jiangxi Geology & Mineral Exploration Bureau Report No. 0900320448.
Li, Y.D., Tao, H., Yao, J., Zhang, Q., 2016. Application of a distributed catchment model to investigate hydrological impacts of climate change within Poyang Lake catchment (China). Hydrol. Res.
Li, P., Feng, Z., Jiang, L., Liu, Y., Xiao, X., 2012. Changes in rice cropping systems in the Poyang Lake Region, China during 2004–2010. J. Geogr. Sci. 22 (4), 653–668.
Lin, J.S., Shi, X.Z., Lu, X.X., Yu, D.S., Wang, H.J., Zhao, Y.C., Sun, W.X., 2009. Storage and Spatial Variation of Phosphorus in Paddy Soils of China. Pedosphere 19 (6), 790–798.
Lin, Y.S., Lin, Y.W., Wang, Y., Chen, Y.G., Hsu, M.L., Chiang, S.H., Chen, Z.S., 2007. Relationships between topography and spatial variations in groundwater and soil morphology within the Taoyuan-Hukou Tableland Northwestern, Taiwan. Geomorphology 90 (1–2), 36–54.
Liu, Y., Wu, G., 2016. Hydroclimatological influences on recently increased droughts in China's largest freshwater lake. Hydro. Earth Syst. Sci. 20, 93–107.
Liu, Z.J., Zhou, W., Li, S.T., He, P., Liang, G.Q., Lv, J.L., Jin, H., 2015. Assessing soil quality of gleyed paddy soils with different productivities in subtropical China. Catena 133, 293–302.
Mei, X.F., Dai, Z.J., Du, J.Z., Chen, J.Y., 2015. Linkage between Three Gorges Dam impacts and the dramatic recessions in China's largest freshwater lake, Poyang Lake. Sci. Rep. 5, 18197. https://doi.org/10.1038/srep18197.
Pan, S.Z., 1996. Characterization of gleyization of paddy soils in the middle reaches of the Yangtze River. Pedosphere 6 (2), 111–119.
Pu, P.M., Cai, S.M., Zhu, H.H., 1994. Three Gorges Project and Lakeshore Environment in the Middle Yangtze River. The Science Publishing Company, Beijing.
Rowell, D.L., 1988. Flooded and poorly drained soils. In: Wild, A. (Ed.), Russell's Soil Conditions and Plant Growth. Longman Scientific and Technical, Essex, pp. 899–926.
Schlichting, E., Schwertmann, U., 1973. Pseudogley and Gley. Verlag Chemie, Weinheim.
Shiratori, Y., Watanabe, H., Furukawa, Y., Tsuruta, H., Inubushi, K., 2007. Effectiveness of a subsurface drainage system in poorly drained paddy fields on reduction of methane emissions. J. Soil Sci. Plant Nut. 53 (4), 387–400.
Singh, S.K. Chandran, P., 2015. Soil genesis and classification, in: Rattan, R.K., Katyal, J. C., Dwivedi B.S. (Eds), Soil Science-An Introduction, first ed. Vedas Sanskrit scripture, pp. 57-96.
Sun, S.L., Chen, H.S., Ju, W.M., Song, J., Li, J.J., Ren, Y.J., Sun, J., 2012. Past and future changes of streamflow in Poyang Lake Basin Southeastern, China. Hydro. Earth Syst. Sci. 16, 2005–2020.
Torbick, N., Salas, W., Xiao, X.M., Ingraham, P., Fearon, M., Biradar, C., Zhao, D.L., Liu, Y., Li, P., Zhao, Y.L., 2011. Integrating SAR and optical imagery for regional mapping of paddy rice attributes in the Poyang Lake Watershed, China. Can. J. Remote Sens. 37 (1), 17–26.
Verheye, W., 2007. Soils and soil sciences. In: Verheye, W. (Ed.), Land Use, Land Cover and Soil Sciences. UNESCO-EOLSS Publishers, Oxford, UK.
Wagner, S., Fersch, B., Yuan, F., Yu, Z., Kunstmann, H., 2016. Fully coupled atmospheric-hydrological modeling at regional and long-term scales: Development, application, and analysis of WRF-HMS. Water Resour. Res. 52 (4), 3187–3211.
Webb, T.H., Lilburne, L.R., 2011. Criteria for Defining the Soil Family and Soil Sibling: the Fourth and Fifth Categories of the New Zealand Soil Classification, second ed. Manaaki Whenua Press, Lincoln, New Zealand.
Wei, Y., Ma, Z.X., Li, J.H., Ma, Y.L., Xie, Z.D., Zhu, Q.M., 2005. Environmental geological survey and evaluation of Poyang Lake Basin in Jiangxi Section of the Middle Reaches of Yangtze River. Geological Survey of Jiangxi Province Report No. 0701100124.
Xiao, Z.B., Rao, Z., Yang, G.F., 2001. Investigation Report on Groundwater Exploitation in Nanchang City. Jiangxi Province, Jiangxi Institute of Geo-Environment Monitoring.
Ye, X.C., Zhang, Q., Bai, L., Hu, Q., 2011. A modeling study of catchment discharge to Poyang Lake under future climate in China. Quatern. Int. 244, 221–229.
Ye, X.C., Zhang, Q., Liu, J., Li, X.H., Xu, C.Y., 2013. Distinguishing the relative impacts of climate change and human activities on variation of streamflow in the Poyang Lake catchment China. J. Hydrol. 494, 83–95.
Zhan, L.C., Chen, J.S., Zhang, S.Y., Li, L., Huang, D.W., Wang, T., 2016. Isotopic signatures of precipitation, surface water, and groundwater interactions, Poyang Lake Basin China. Environ. Earth Sci. 75 (19), 1–14.
Zhang, G.L., Xiao, X.M., Biradar, C.M., Dong, J.W., Qin, Y.W., Menarguez, M.A., Zhou, Y.T., Zhang, Y., Jin, C., Wang, J., Doughty, R.B., Ding, M.J., Moore, B., 2017. Spatiotemporal patterns of paddy rice croplands in China and India from 2000 to 2015. Sci. Total Environ. 579, 82–92.
Zhang, L.T., 2008. Investigation Report on Quaternary Geology in Poyang Lake Basin. Jiangxi Province, Jiangxi Geology & Mineral Exploration Bureau Report No 0900324853.
Zhang, Q., Werner, A.D., 2009. Integrated surface-subsurface modeling of Fuxianhu Lake catchment, Southwest China. Water Resour. Manage. 23, 2189–2204.
Zhang, Q., Xiao, M.Z., Li, J.F., Singh, V.P., Wang, Z.Z., 2014. Topography-based spatial patterns of precipitation extremes in the Poyang Lake basin, China: Changing properties and causes. J. Hydrol. 512, 229–239.